Shell Model applications in nuclear astrophysics

Gabriel Martínez-Pinedo

13th International Spring Seminar on Nuclear Physics

Sant'Angelo d'Ischia, May 16-20, 2022

Helmholtz Forschungsakademie Hessen für FAIR

European Research Council
Established by the European Commission

Stellar evolution

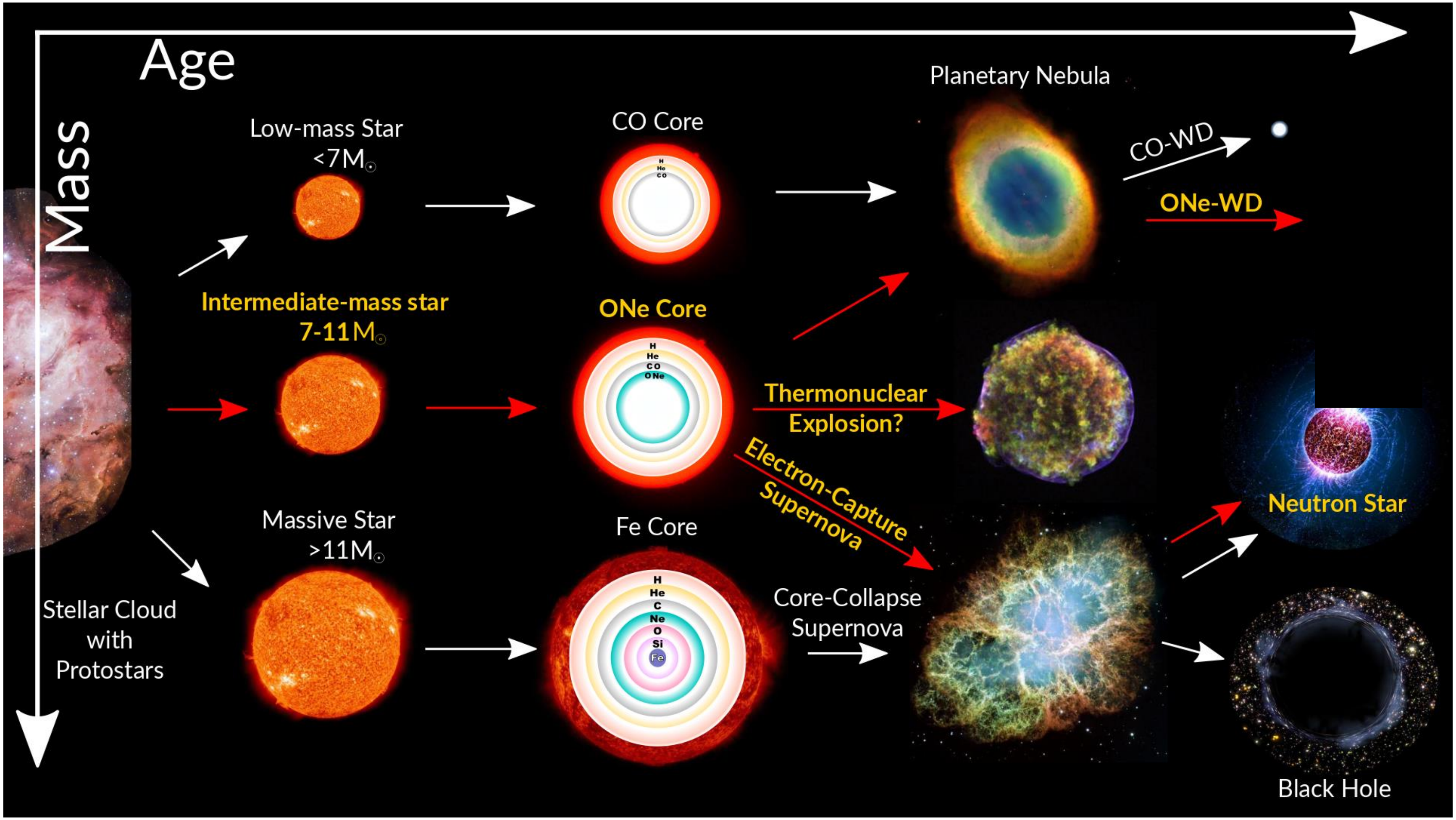

Late phases of evolution determined by electron capture processes. They remove electrons from stellar plasma reducing the pressure support and determine the temperature evolution.

Electron capture regimes

Several regimes are possible depending on the astrophysical conditions:

- Low temperatures: sensitive to individual transitions. Rates very sensitive to density. Intermediate mass stars
- Moderate temperatures: sensitive to several low lying Gamow-Teller transitions. Contribution of a few excited states. Early collapse phase.
- High temperature and densities: sensitive to GT and forbidden resonances. Finite temperature calculations necessary. Late collapse phase.

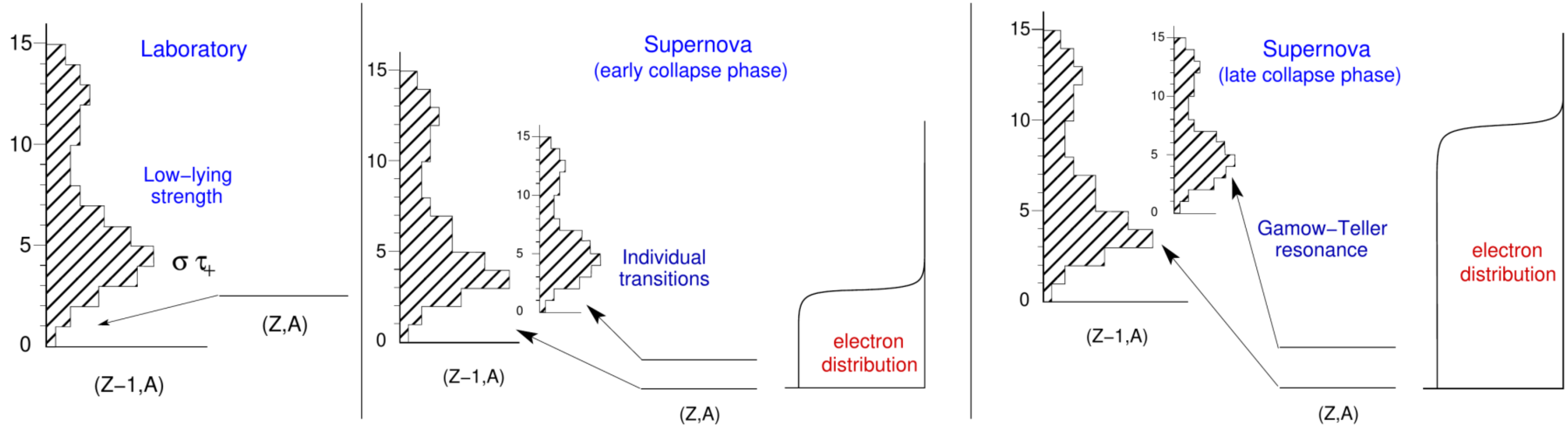

Intermediate mass stars: late time evolution

- After the formation of the ONeMg core, shell burning keeps adding mass to the core. With increasing density electron capture processes become possible.
- At some point Oxygen burning may eventually take place.
- There is a critical density such as for lower values burning leads to a thermonuclear supernova while for higher values the end product is a neutron star after core-collapse.
- Two main uncertainties: weak processes and convective instabilities.

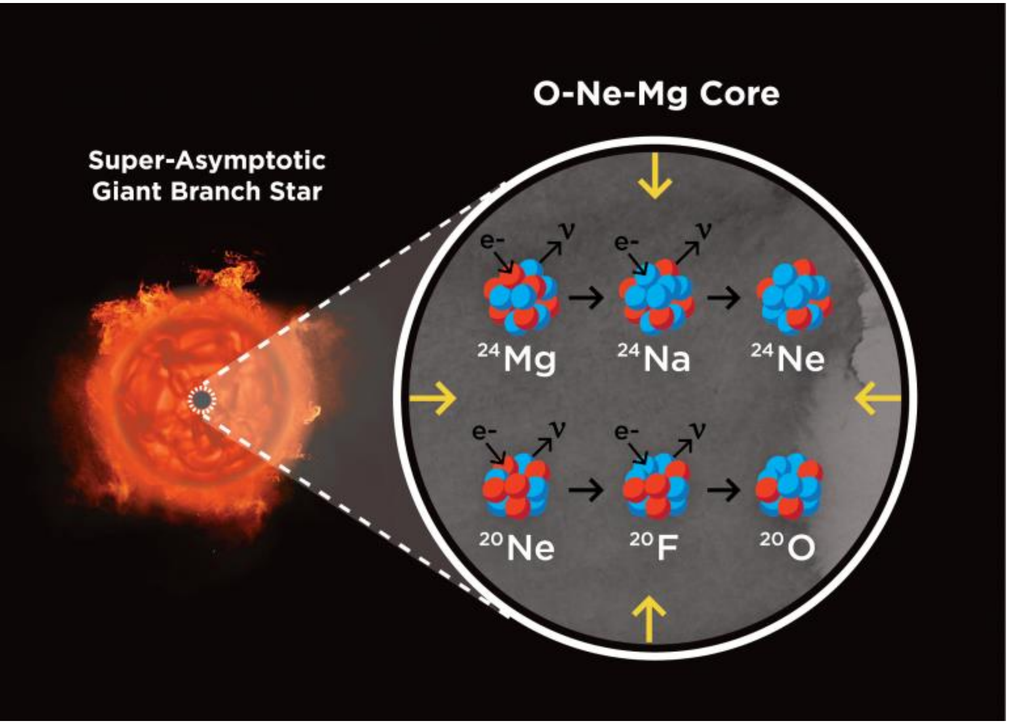

Jones et al, ApJ 772, 150 (2013)

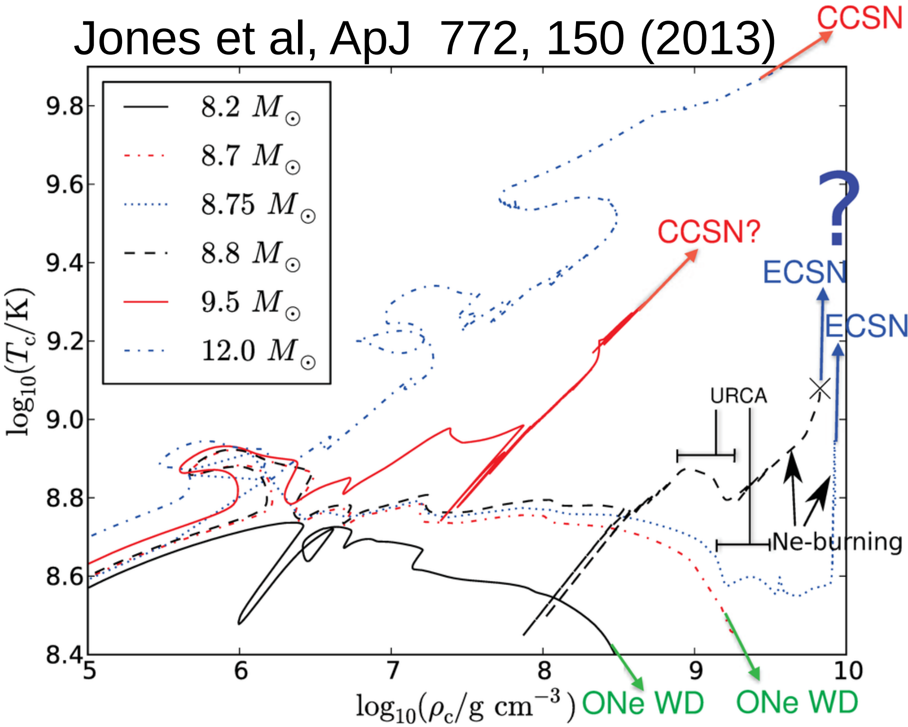

Urca pairs: cooling vs heating

mass parabola for isobaric chain

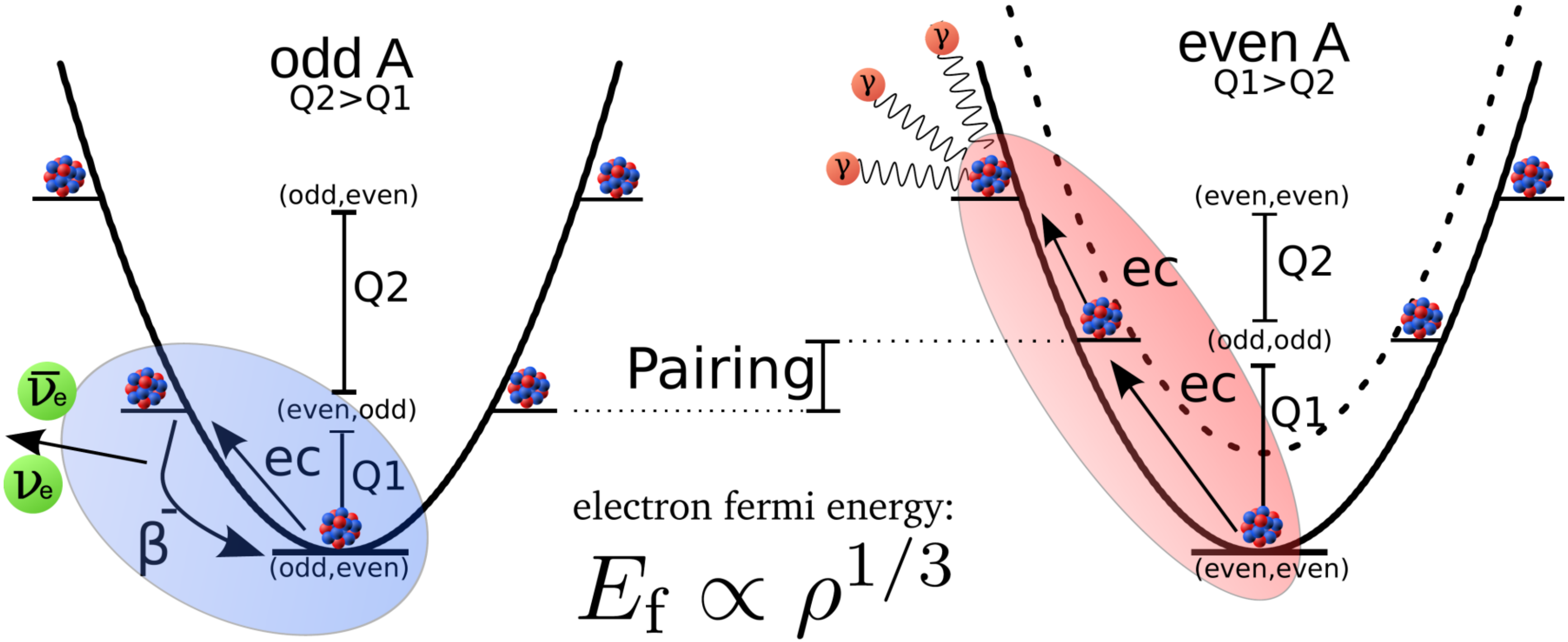

Urca cooling

$$(\text{A,Z}) + e^- = (\text{A,Z-1}) + \nu_e$$
$$(\text{A,Z-1}) = (\text{A,Z}) + e^- + \bar{\nu}_e$$

heating

$$(\text{A,Z}) + e^- = (\text{A,Z-1}) + \nu_e$$
$$(\text{A,Z-1}) + e^- = (\text{A,Z-2})^* + \nu_e + \gamma$$

Figure from Heiko Möller, PhD, 2016

Intermediate mass stars: role of second forbidden transitions

- All relevant allowed transitions identified and experimetally known except for two forbidden transitions:

$$^{20}\mathrm{Ne}\,(0^+,\mathrm{gs}) \rightarrow {}^{20}\mathrm{F}\,(2^+,\mathrm{gs}) \qquad {}^{24}\mathrm{Na}\,(4^+,\mathrm{gs}) \rightarrow {}^{24}\mathrm{Ne}\,(2^+)$$

- Suggested to have an important role for electron capture on ^{20}Ne and ^{24}Mg [GMP et al, PRC 89, 045806 (2014)]

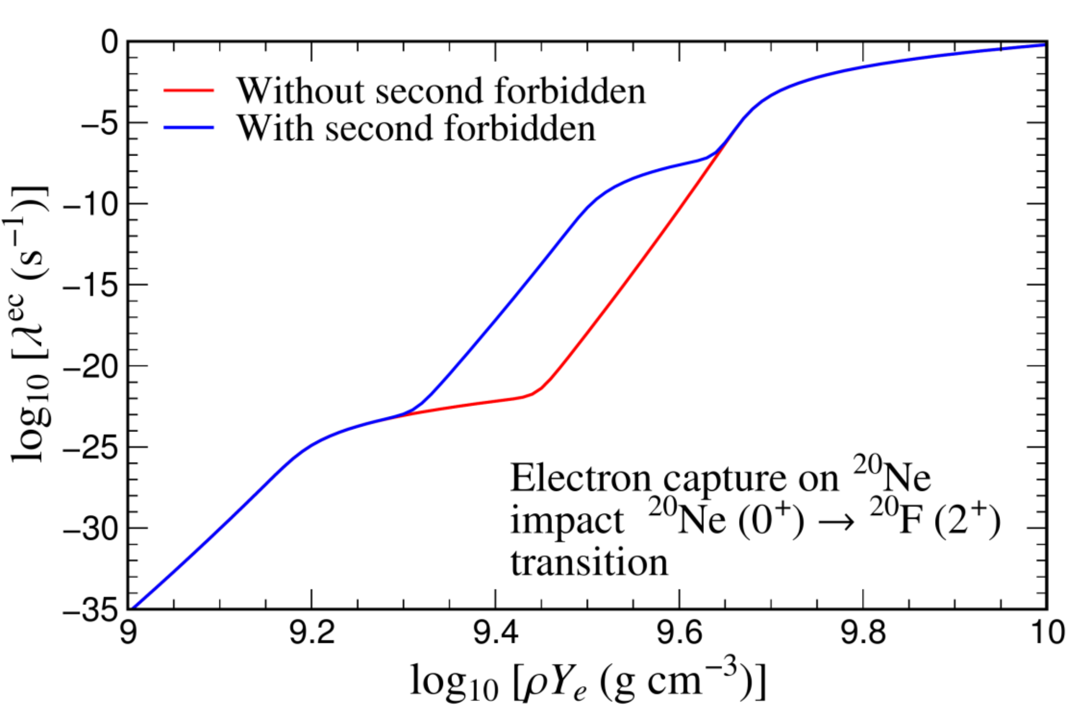

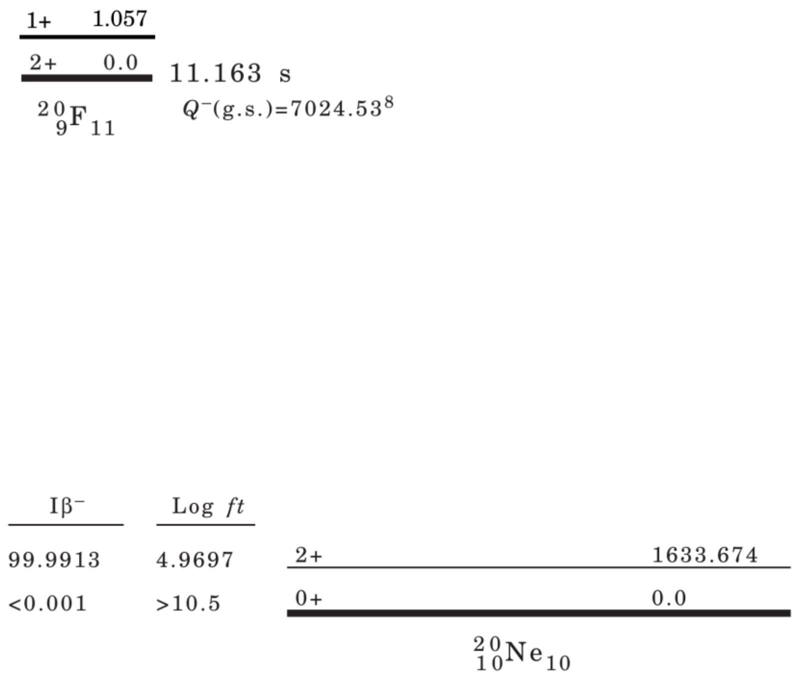

Second forbidden transition ^{20}Ne

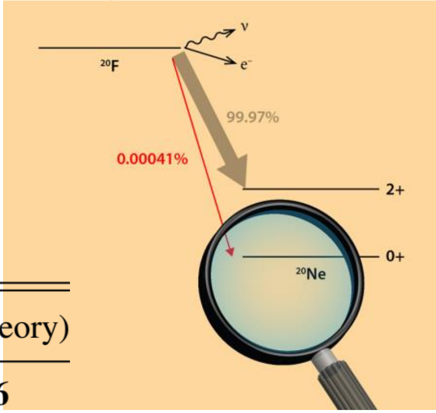

- Measured at IGISOL/JYFL Jyväskylä [Kirsebom et al, PRL 123, 262701 (2019), PRC 100, 065805 (2019)]
- One of the strongest second-forbidden transitions ever measured

$$\lambda \sim \int C(E_e)F(Z,E_e)p_eE_eE_\nu^2dE_e \qquad {}^VF_{211}^0 \sim [\boldsymbol{\alpha}\otimes \boldsymbol{r}]^2 \to [\boldsymbol{p}\otimes\boldsymbol{r}]^2 \,/\, M$$

Shape	g_A	χ^2/N	p value	b_β ($\times 10^{-5}$)	log ft	log ft (theory)
SM+CVC+E2	**−1.27**	**1.193**	**0.080**	**0.41(8)(7)**	**10.89(11)**	**10.86**
SM+CVC+E2	−1.0	1.190	0.083	0.43(8)(7)	10.88(11)	10.91
SM	−1.27	1.190	0.083	0.90(17)(14)	10.55(11)	10.76
SM	−1.0	1.189	0.083	0.95(18)(15)	10.53(11)	10.73
allowed	–	1.192	0.081	1.10(21)(18)	10.46(11)	–

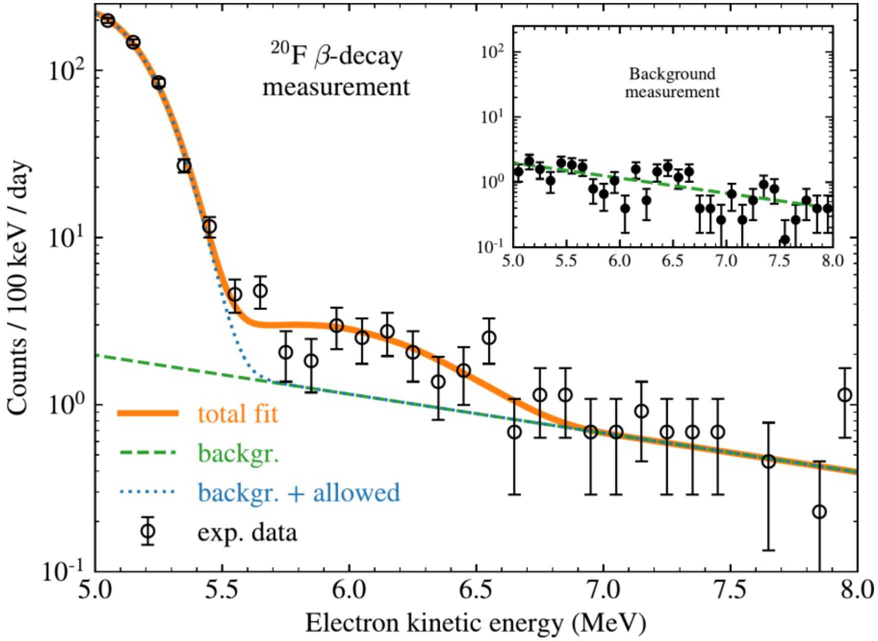

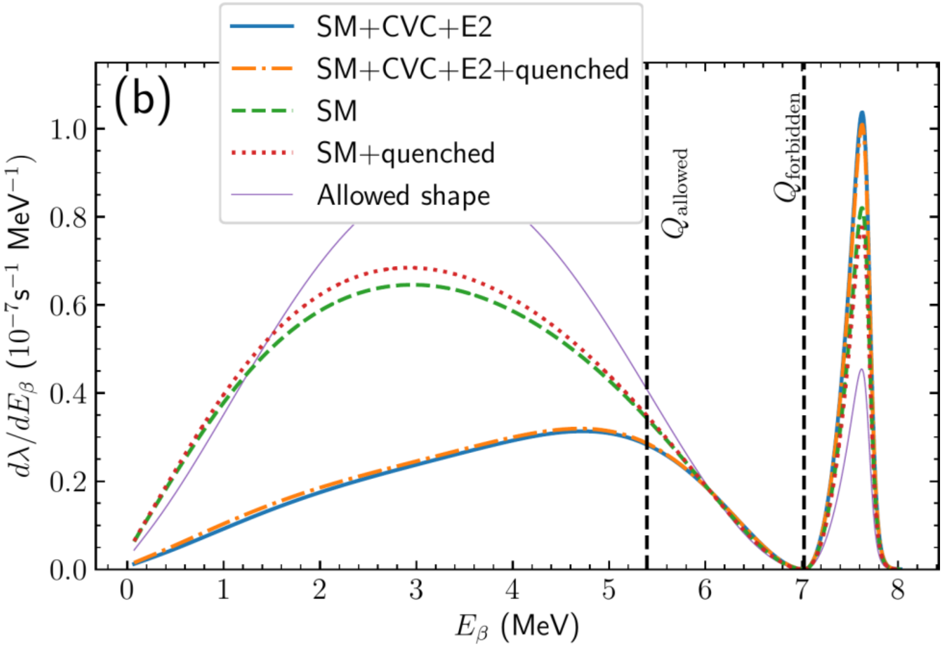

Impact electron capture rate on evolution

- Rate fully based on experimental information
- Unique case: rate dominated by a forbidden transition.
- Main nuclear uncertainty resolved
- New rate favors ignition of Oxygen at lower densities

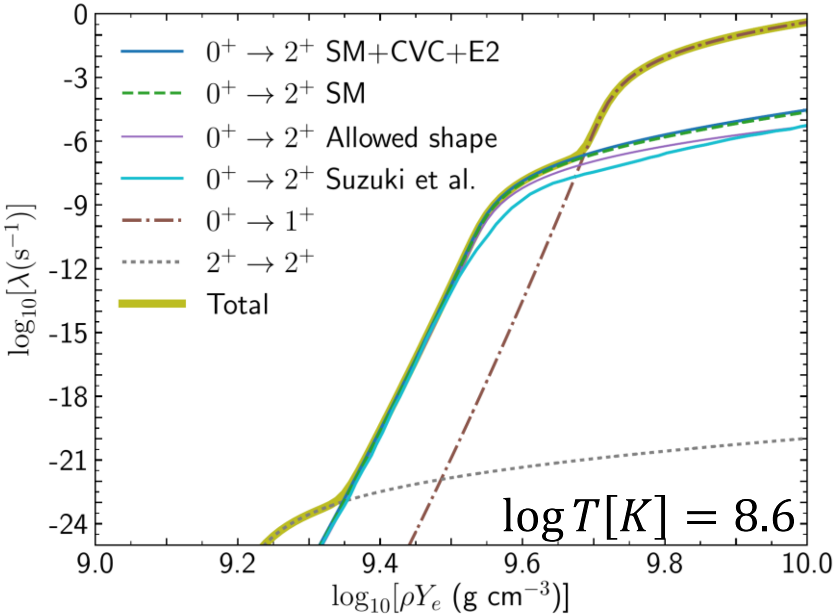

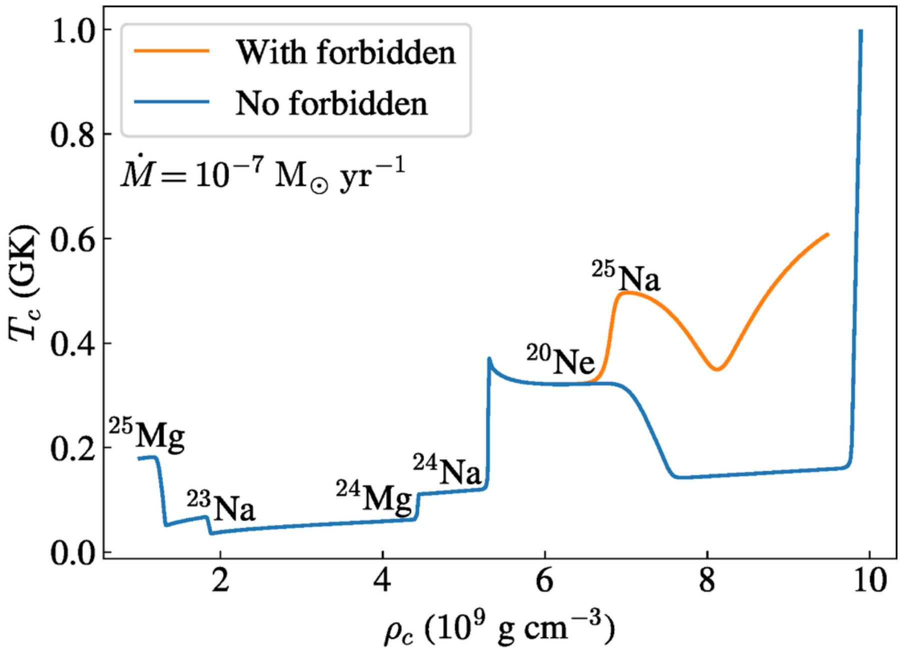

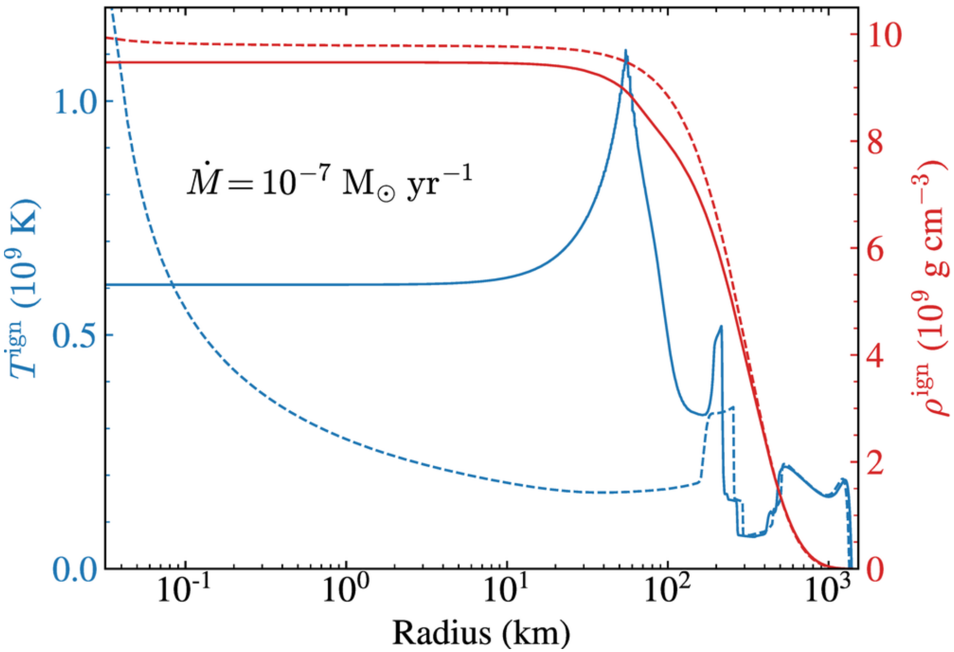

Final outcome

- Oxygen ignites at lower densities favoring a thermonuclear supernova. Main nuclear uncerta
- 3D simulations by Jones and Röpke produce a thermonuclear explosion with a ONeFe white dwarf remnant

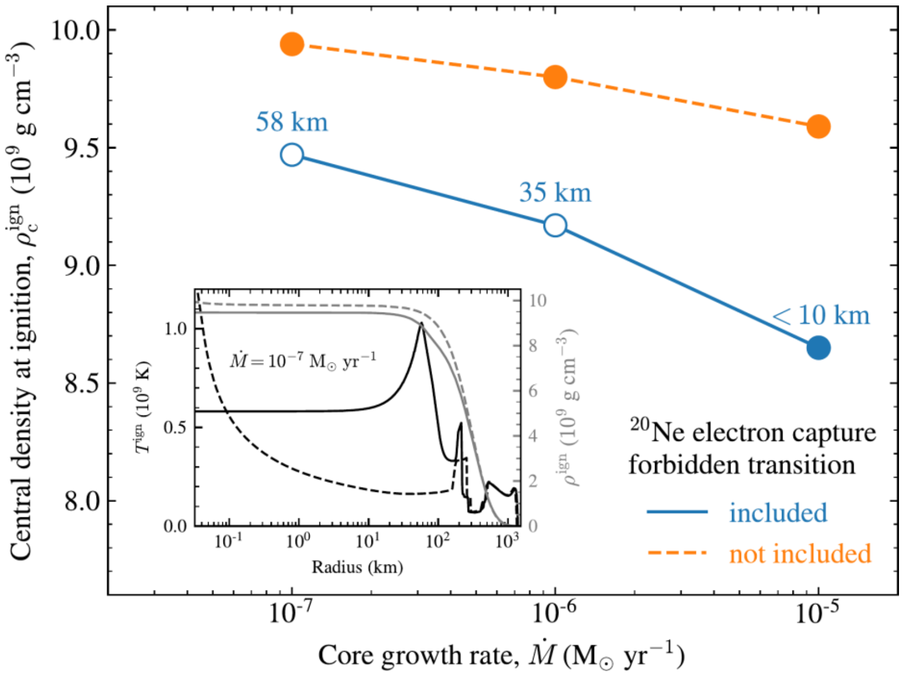

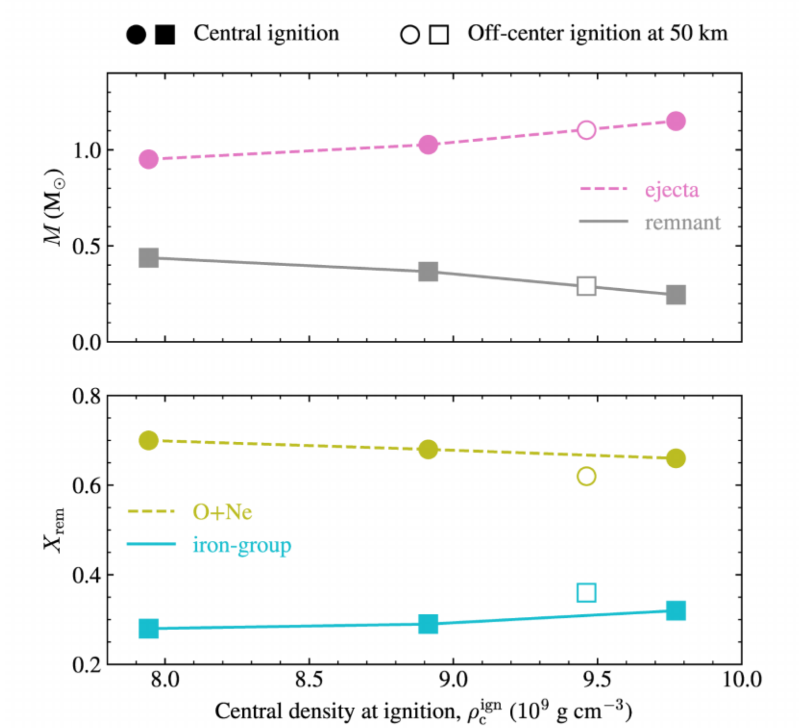

- Role of convection remains uncertain [Leung et al ApJ 889 34 (2020)]. Second forbidden transition on ^{24}Na may trigger convective instabilities [Schwab et al, MNRAS 472, 3390 (2017), Strömberg et al, PRC 105, 025803 (2022)]
- Recently a supernova candidate observed [Hiramatsu, Nature Astron. 5, 903 (2021)

Electron capture: early collapse

- During and after Silicon burning electron capture dominated by Iron group nuclei.
- Well described by $0\hbar\omega$ pf shell model calculations. [Langanke, GMP, NPA 673, 481 (2000)]
- Constrained by charge-exchange experiments

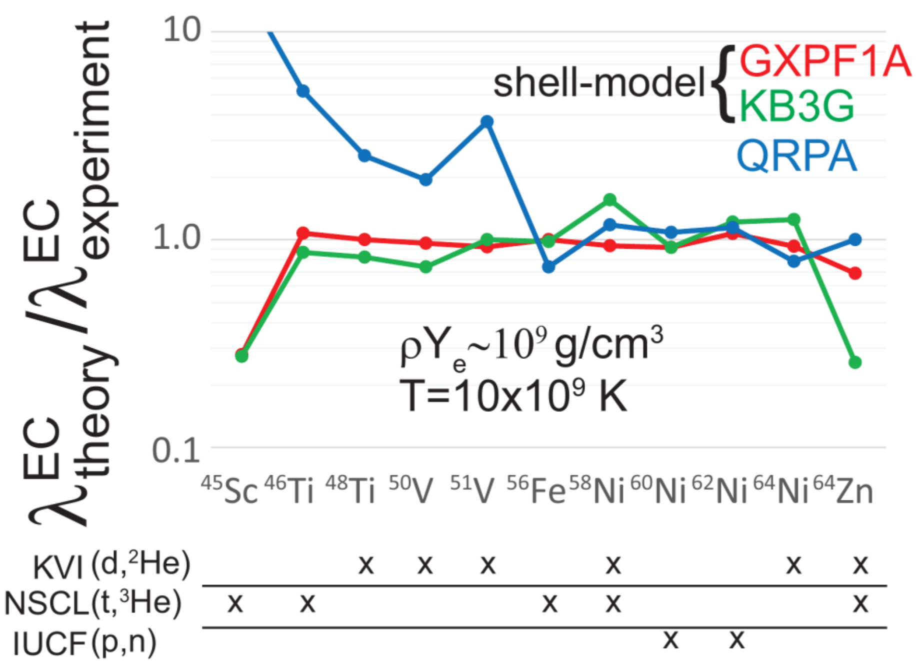

Langanke, GMP & Zegers, RPP 84, 066301 (2021)

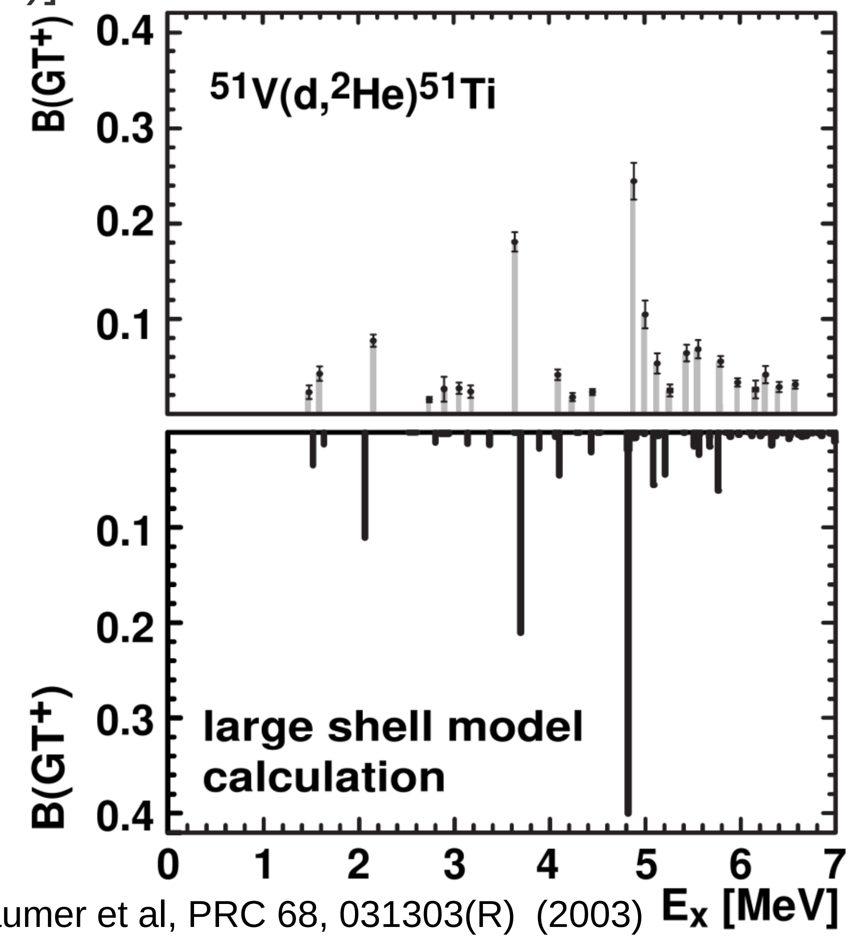

Bäumer et al, PRC 68, 031303(R) (2003)

Electron capture: late collapse

- With increasing density composition shifts to neutron-rich nuclei and core temperatures are around 1 MeV.
- Description nucleus at finite temperature (Shell-Model Monte Carlo)

Unblocking GT strength

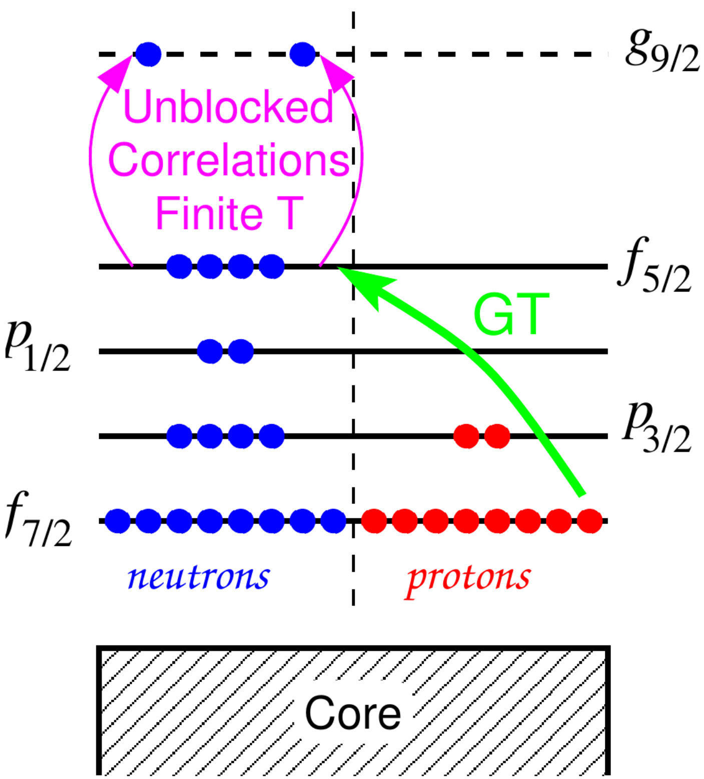

Langanke, et al, PRL 90, 241102 (2003)
Juodagalvis, et al, NPA 848, 454 (2010)

SMMC Rates are mainly sensitive to Q-value

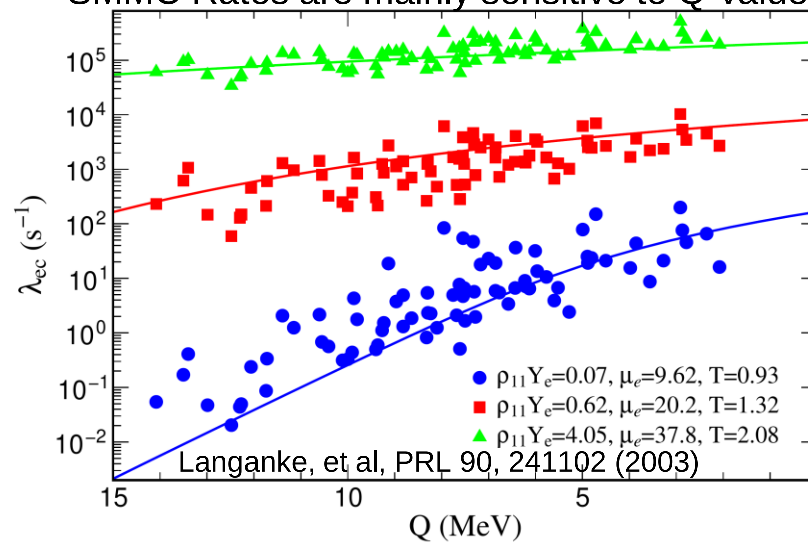

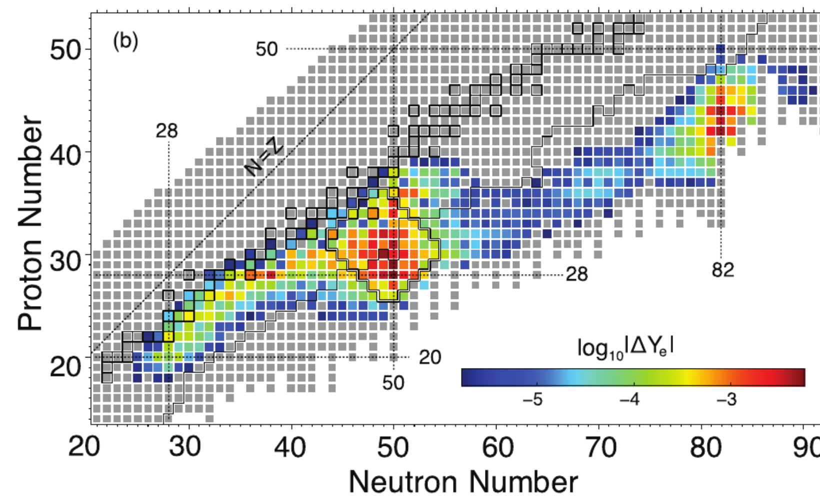

Sullivan et al, ApJ 816, 44 (2016)

Electron capture around N=50

- GT+ measurements for 86Kr [Titus et al, PRC 100, 045805 (2019)] and 88Sr [Zamora et al, PRC 100, 032801(R) (2019)] show very little strength. Strong blocking for the ground state.
- At astrophysical temperatures nucleus is thermally excited at energies ~ 10 MeV.

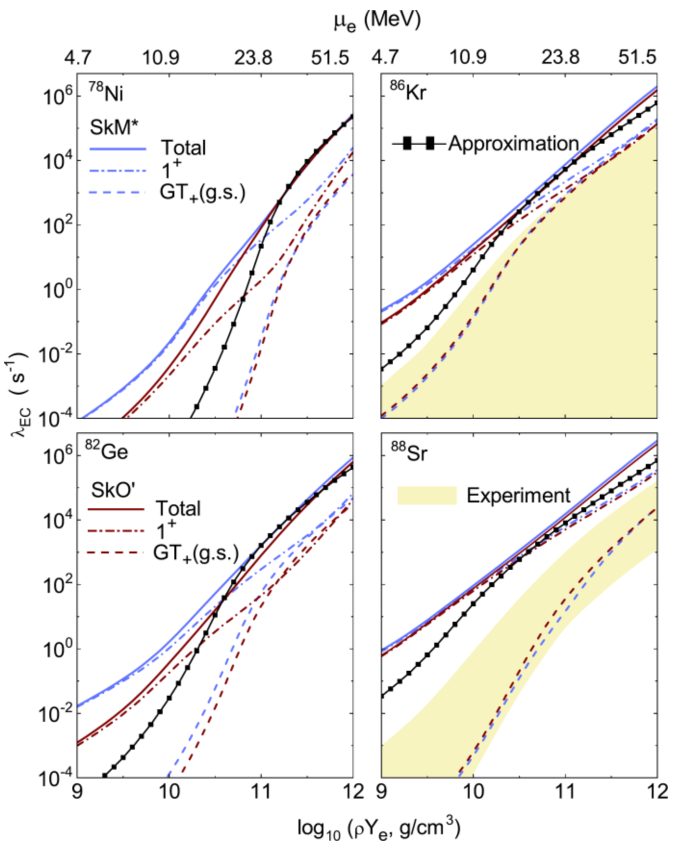

Similar thermal enhancements obtained by Litvinova & Robin, PRC 103, 024326 (2021) Giraud et al, PRC 105, 055801 (2022)

Giraud et al uses different theoretical approaches showing that differences in rates lead to very small changes in core-collapse evolution

Thermal-QRPA: Dzhioev, et al, PRC 101, 025805 (2020)

R process nuclear needs

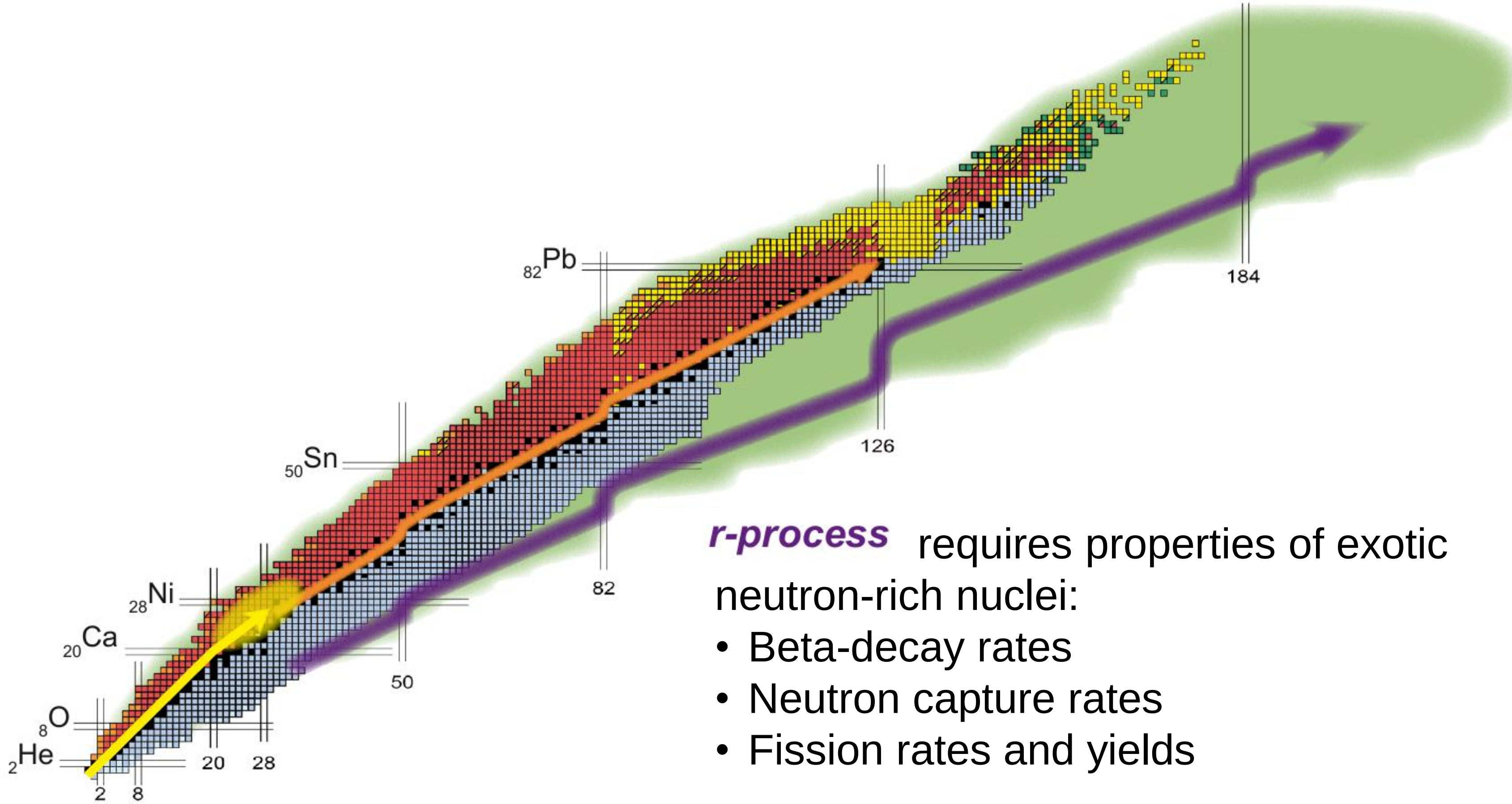

r-process requires properties of exotic neutron-rich nuclei:

- Beta-decay rates
- Neutron capture rates
- Fission rates and yields

Shell Model calculation beta-decays

- Shell Model calculations so far are restricted to magic nuclei around N=50, 82 and 126 [Zhi et al, PRC 87, 024803 (2013), Suzuki et al, PRC 85, 015802 (2012)]
- Assume a neutron shell closure configuration for initial states

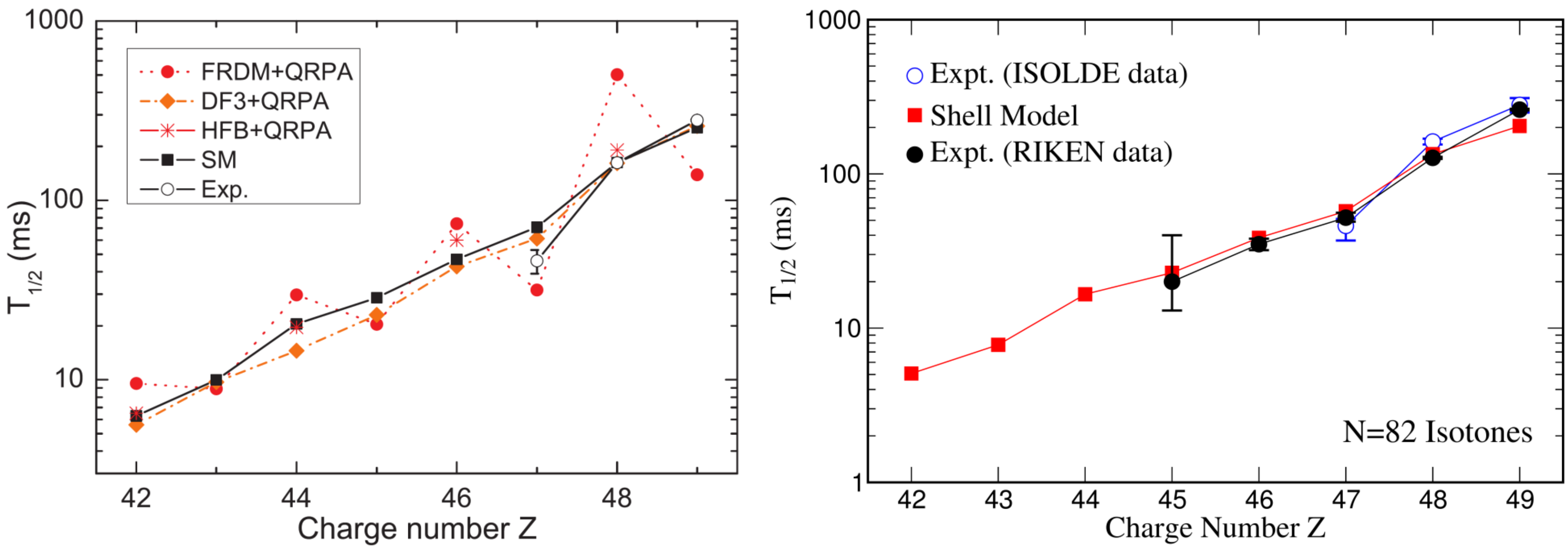

Point to an increasing role of forbidden transitions with increasing mass. Particularly at N=126.

Global β decay calculations in QRPA

FF contribution to the rates in different QRPA's:

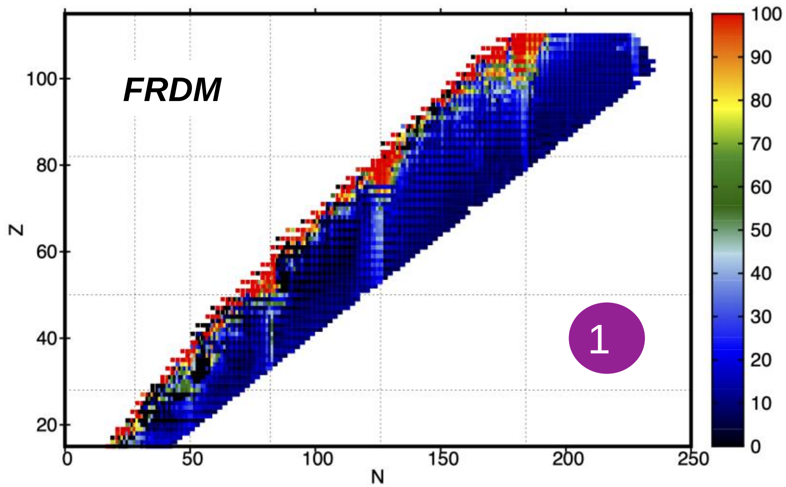

1. *QRPA approach based on FRDM for the Gamow-Teller + gross theory for the first-forbidden*

   Moeller, Pfeiffer, Kratz, PRC 67, 055802 (2003)
   https://t2.lanl.gov/nis/data/astro/molnix96/tbeta.html

2. *Relativistic QRPA based on D3C* functional*

   Marketin, Huther, Martínez-Pinedo PRC 93, 025805 (2016)

3. *Non relativistic QRPA based on Skyrme functional SKO'*

   Ney, Engel, Li, Schunck PRC102, 034326 (2020)

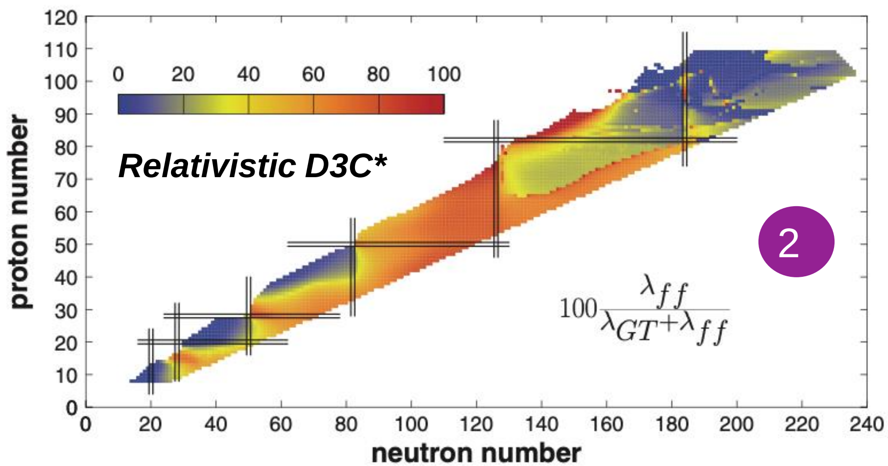

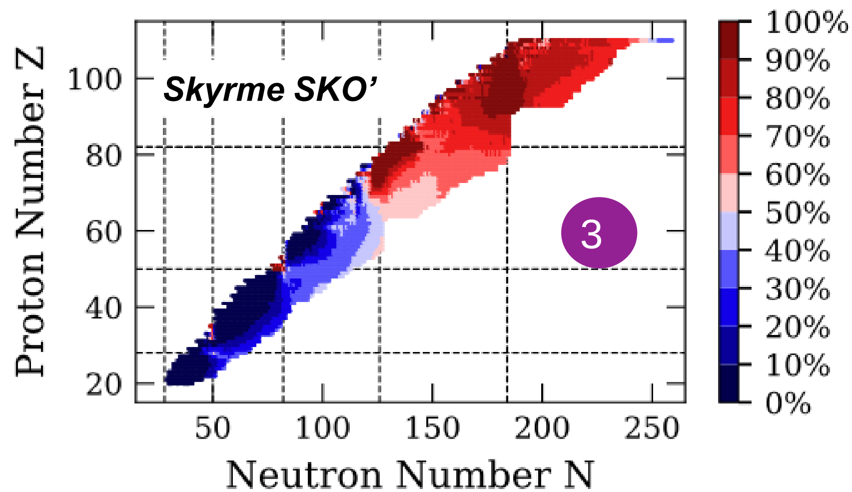

β decay in QRPA

Comparison of the total half-lives in different QRPA's:

Ney et al. PRC 102, 034326 (2020)

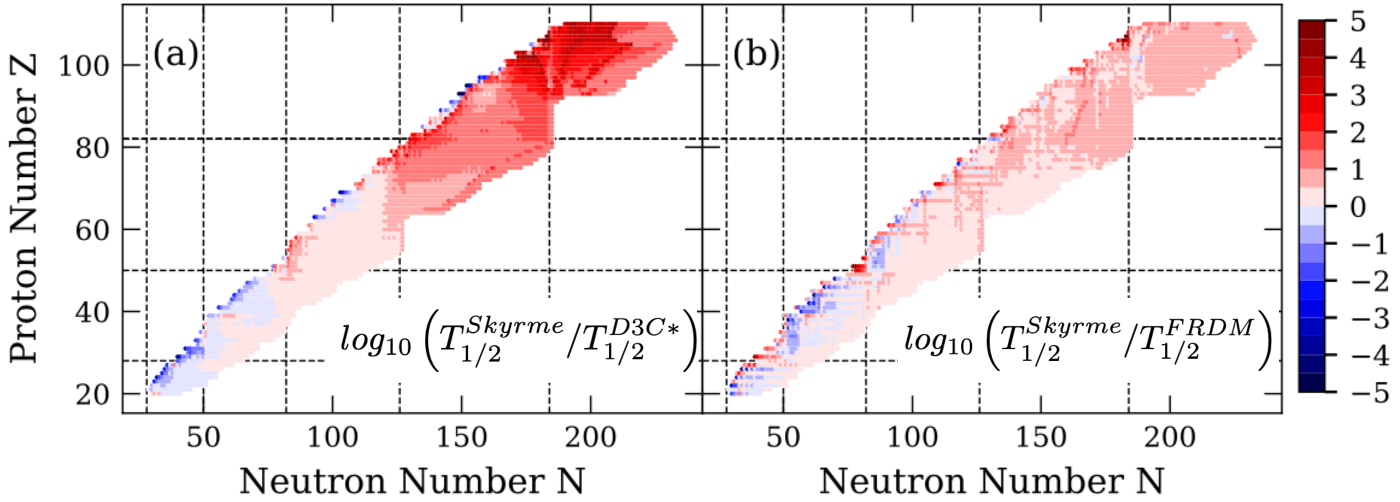

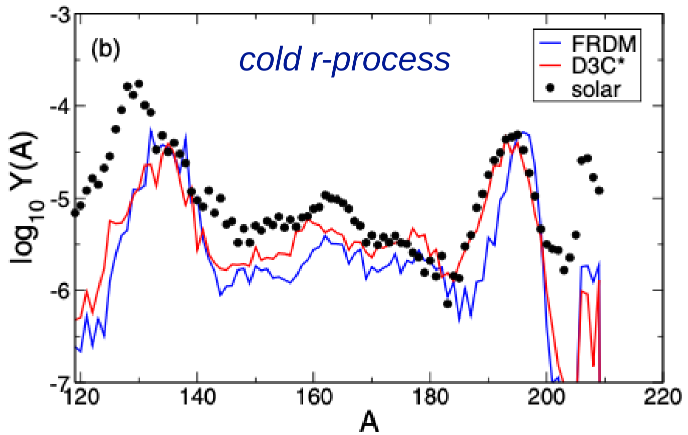

Marketin, Huther, Martínez-Pinedo PRC 93, 025805 (2016)

- ✶ ~ agreement between the 3 approaches below N<126
- ✶ Above N>126 the relativistic QRPA predicts considerably shorter half-lives than the other ones

⇒ broadening of the third peak (A~195) towards lower masses

Beyond QRPA: Relativistic Nuclear Field Theory (RNFT)

Degrees of freedom in RNFT:

=

- ✶ relativistic effective mesons — π σ ω ρ (m ~ 140-800 MeV) *quantum hadrodynamics*
- ✶ relativistic nucleons — p n (S_n ~ 10 MeV)
- ✶ phonons (collective vibrations of the nucleus)

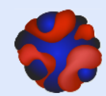

(E ~ few MeV)

C. Robin and E. Litvinova
PRC 98, 051301 (2018);
EPJA 52, 205 (2016);

systematic expansion in the PVC vertex

Nucleonic motion =

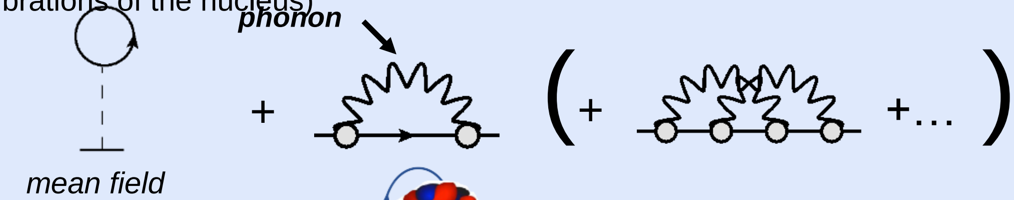

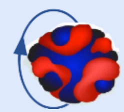

particle-vibration coupling (PVC)

Effective NN interaction =

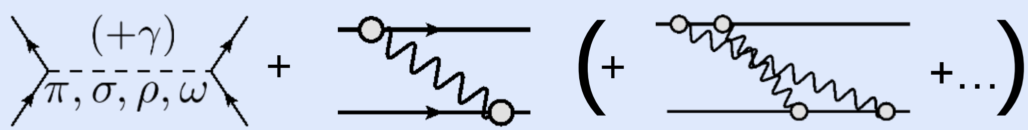

1p-1h (QRPA) *2p-2h* *3p-3h (future)* *…*

Advantages:

✦ *Applicability up to heavy/superheavy masses to be useful for astrophysical applications*

✦ *while allowing for a precise description of nuclear phenomena*

Particle-Vibration Coupling effect on β decay of r-process nuclei

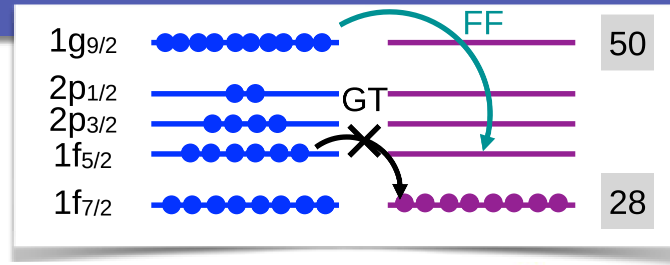

★ **β-decay of isotonic chain N=50**

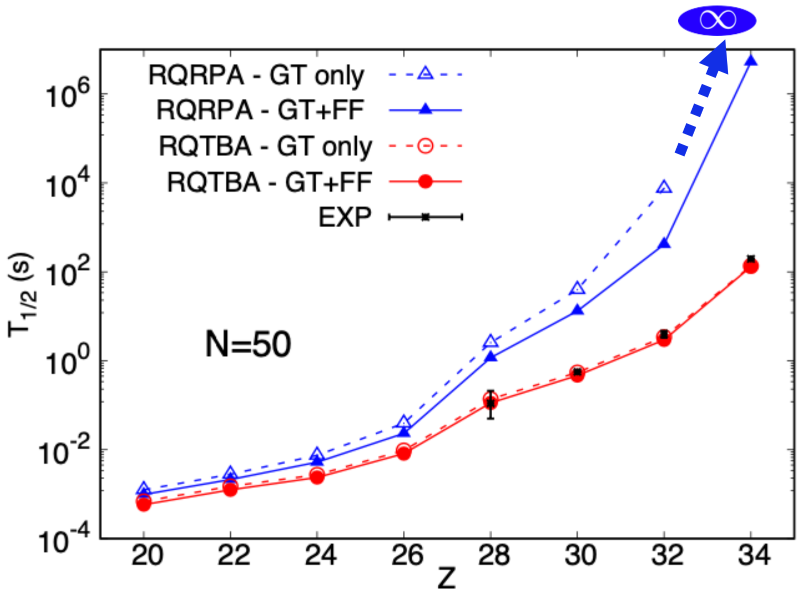

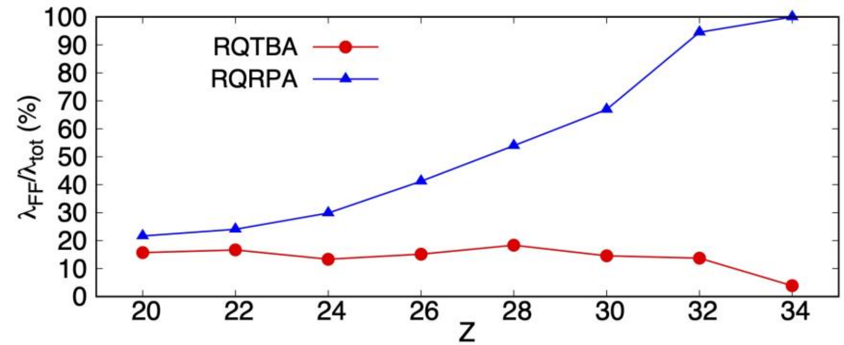

- *The low-energy GT transition is blocked for Z≥28.*
- *In RQRPA, other GT transitions are near the Q value.*
- *With correlations, they are lowered in energy due to fragmentation.*

Comparison to other approaches:

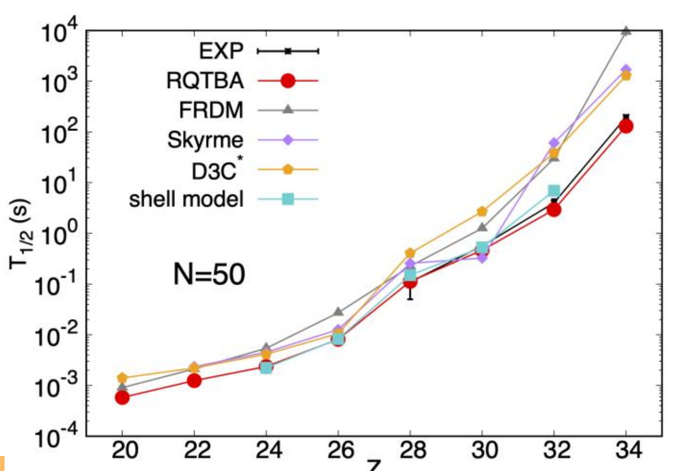

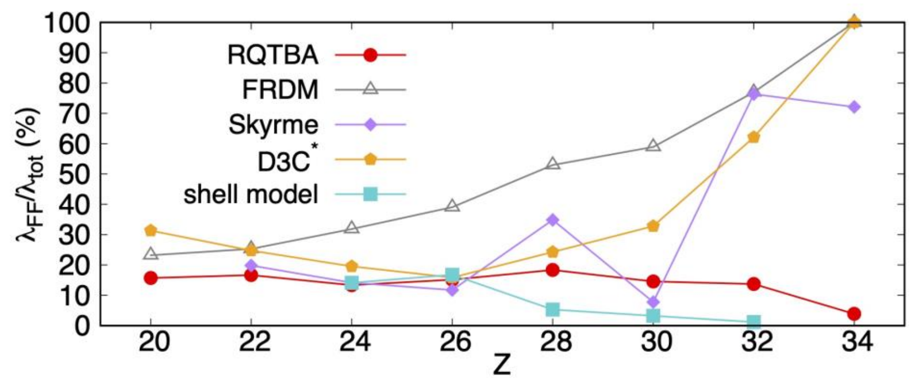

C. Robin, GMP, in preparation

★ **β-decay of isotonic chain N=126**

Comparison to other approaches:

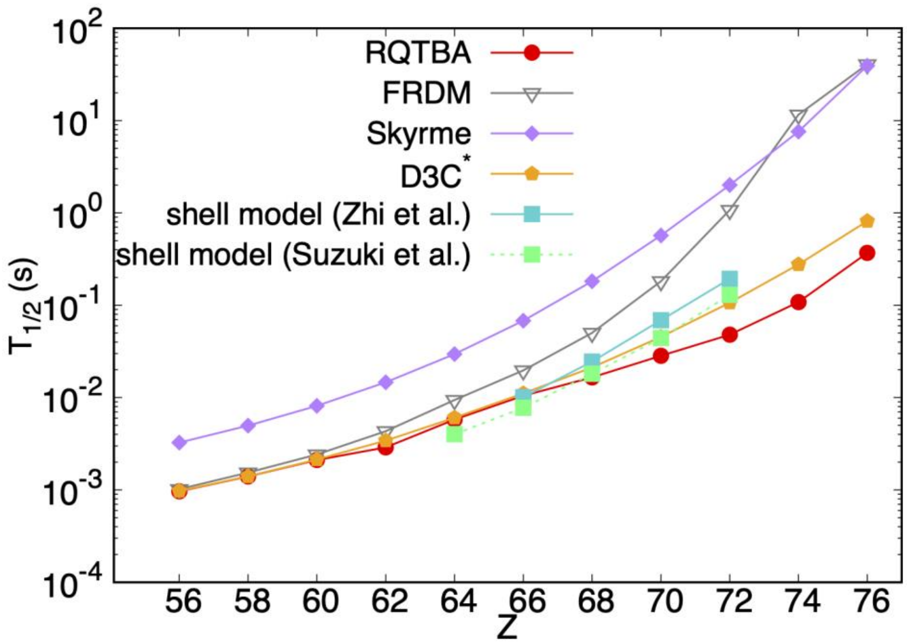

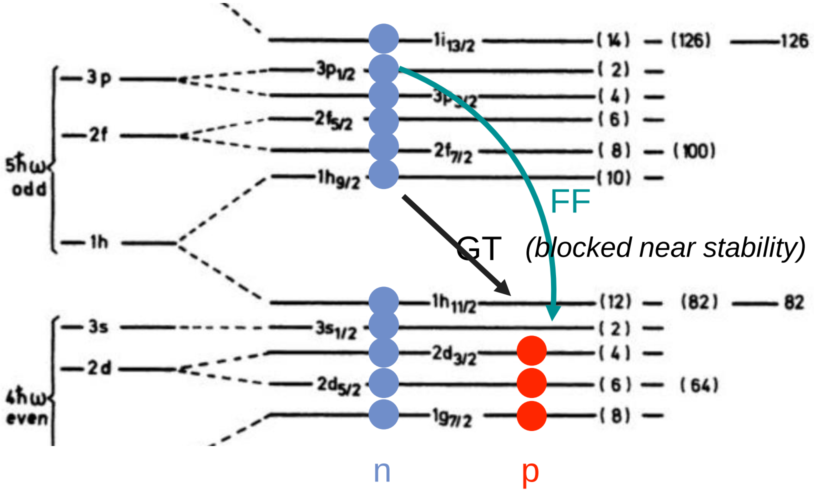

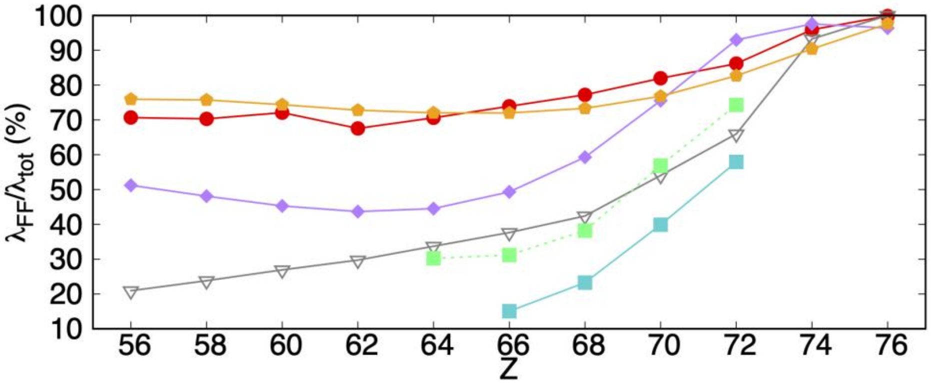

C. Robin, GMP, in preparation

→ no agreement on the contribution of FF transitions far from stability

Particle-Vibration Coupling effect on β decay of r-process nuclei

→ Contributions of the 0⁻ first-forbidden modes:

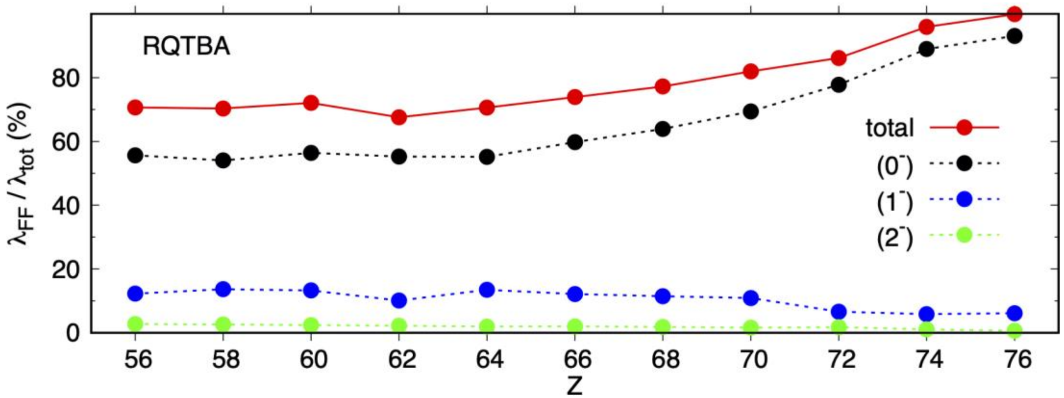

⇒ The decay occurs dominantly via 0⁻ FF transitions

✴ *spin-dipole (SD) modes*

$$\mathcal{O}_{SA} \propto (\boldsymbol{\sigma}.\boldsymbol{r})\ \tau_-$$

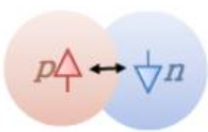

L=1 , S=1, J=0

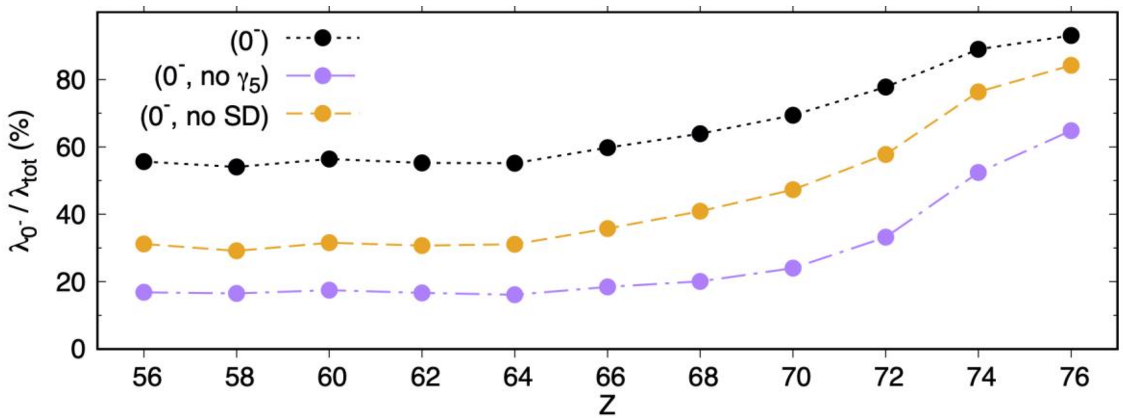

✴ relativistic contributions

$$\mathcal{O}_{RA} \propto \gamma_5 \tau_-$$

⇒ Relativistic effects appear to be the most important

C. Robin, GMP, in preparation

Summary

- Weak rates relevant for intermediate mass star evolution are fully constrained by experimental information.
- Role of convection needs to be addressed to determine final outcome: thermonuclear or core-collapse explosions
- Electron capture rates for core-collapse around N=50 strongly enhanced due to thermal effects.
- Role of forbidden transitions for beta-decays of r-process heavy nuclei needs to be addressed.
- Experimental information is fundamental

Collaborators: A. A. Dzhioev, S. Jones, O. S. Kirsebom, K. Langanke, F. Nowacki, **C. Robin**, **D. F. Strömberg**, F. K. Röpke, R. Zegers.